HIGH POWER, HIGH BRIGHTNESS PROTON ACCELERATORS*

YONG YUNG LEE
Brookhaven National Laboratory
Upton, New York 11973 USA
E-mail : yyl@bnl.gov

Received July 15, 2005

The development of accelerator science and technology has been accommodating ever increasing demand from scientific community of the beam energy and intensity of proton beams. The use of high-powered proton beams has extended from the traditional application of nuclear and high-energy physics to other applications, including spallation neutron source replacing nuclear reactor, nuclear actinide transmutation, energy amplification reactors. This article attempts to review development of proton accelerator, both linear and circular, and issues related to the proton beam energy, intensity as well as its output power. For related accelerator physics and technical review, one should refer to the recent article in the Reviews of Modern Physics [1]

KEYWORDS : Proton, Accelerator, High Intensity, High Power, Linac, Synchrotron

1. HISTORICAL REVIEW

1.1 Accelerator

Proton accelerators were originally developed for nuclear physics experiments as an alternative to radioactive source or cosmic rays. From the earliest days, the energy of the proton has been the most important design parameter of the accelerator builders. As early proton accelerators one can name the **Van de Graaff**[2] and **Cockcroft-Walton**[3] devices. They are electrostatic machines, of which their energy is limited to less than 1 MeV for the Cockcroft-Walton and to the order of ten MeV for the Van de Graaff. However, the Van de Graaff is unable to provide as much proton current as a Cockcroft-Walton limited by the capability of the high voltage generator. The output energy of these devices is limited to the voltage that could be generated, which is too low for some of the experiments of interest. A new method of acceleration was needed.

Acceleration of charged particle using a radio frequency source was first proposed by Ising[4] and known as resonant acceleration. Using Ising's idea, Wideroe built the first demonstration linear accelerator[5]. With the technology of the time, the linear accelerator or **linac** was rather difficult to build and there was no further development for some time. Inspired by Wideroe's written account and the fact that time required to make complete circle in constant magnetic field being independent of energy, the fixed frequency **cyclotron** was invented by Lawrence[6] and the first demonstration cyclotron was built by Livingston in 1931. The cyclotron, however, has also an energy limitation due to the relativistic time dilation effect. The cyclotron works in the energy range where the momentum of the proton is approximately proportional to the velocity. Even with the development of the synchrocyclotron, it was clear that a new idea was needed to accelerate to higher energy and satisfy the experimental requirements.

At this point, we must mention the story of the **betatron**. A betatron accelerates the beam by changing the magnetic flux enclosed by the beam path or orbit. If the ratio of the guide field for the beam and the magnetic field enclosed by the orbit is limited to a two to one ratio, the beam particles can be accelerated by simply increasing the magnetic field. The Norwegian physicist Wideroe suggested this "betatron acceleration" mechanism[7] and called it a "Strahlung transformator" or "ray transformer" because the particle orbit acts like a secondary winding of a transformer while the magnetic coil acts as primary. This simple device is independent of the relativistic effect and only dependent on the geometry of the magnet, and ideal for accelerating electrons as relativistic effect prevents electron cyclotron of any significant energy. Wideroe wrote his idea in his notebook, but his attempt to build a demonstration accelerator failed. Years later, when Kerst[8] independently invent and built the first betatron, Wideroe mentioned his notebook to Kerst. The limit of the betatron top energy is

* Work supported by US Department of Energy

Table 1. Comparison of Steel Weights in Synchrotrons

Laboratory	Synchrotron	Type	Energy(GeV)	Weight of Steel(Tons)	Year completed
Brookhaven	Cosmotron	Weak Focusing	3	2000	1952
Berkley	Bevatron	Weak Focusing	6	9700	1954
Dubna, USSR	Synchrophasotron	Weak Focusing	10	36000	1957
CERN	PS	Strong Focusing	28	3000	1959
Brookhaven	AGS	Strong Focusing	33	4000	1960
IHEP, USSR	Serpukhov PS	Strong Focusing	76	20000	1967
FNAL	Main Ring	Strong Focusing	400	9000	1972

the magnetic field strength and the magnet size that one can practically build. The description of the motion of the particle in a betatron was published in 1941 and called "betatron oscillation"[9]. The name has been universally adopted for modern day accelerators.

In the **synchrotron**[10,11] the guide field increases with the energy and keeps the orbit constant, and acceleration is accomplished by a separate radio frequency(RF) cavity, which is synchronized with the orbital frequency. While the magnetic guide field controls and focuses transverse motion, electric field from radio frequency(rf) focuses the particles longitudinally[9,10]. The first proton synchrotron to accelerate to the GeV range was the 3 GeV Cosmotron at Brookhaven National Laboratory in 1952. One of the most important developments for synchrotrons was the "**strong focusing**" or "alternating-gradient(AG) focusing" concept by Courant, Snyder and Livingston[12,13], also independently by Christofilos[14]. Up to this point, the only mechanism to focus and contain the circulating beam in the transverse plain was to provide a constant gradient in the guide field (Cosmotron, Bevatron) or edge focusing (ZGS). In a weak focusing synchrotron, which the above machines were, the guide field decreases with increasing orbital radius to contain the beam vertically. Its gradient is constant throughout the circumference of the machine, and sensitivity to gradient error is very severe. Also the aperture required to contain the beam is large and the magnet becomes large and costly. Table I shows the amount of steel used to construct the synchrotrons constructed in the 1950's and 60's. One can see a huge difference between strong and weak focusing synchrotron structures.

Synchrotrons have now become the main accelerator for the ever expanding energy frontier. Figure 1 shows the energy and the year completed of proton accelerators (simplified Livingston Chart). As can be seen from the figure, after 1970's it became clear the rate of energy frontier growth could no longer be sustained with conventional fixed target machines. The circumference of synchrotrons required to accelerate to higher energies became too large even for superconducting magnets. Colliding beam devices became the way to push the energy frontier further. In the figure the collider energies are represented with that of an equivalent fixed target accelerator.

Having given way to the circular accelerators in the 1930s, the linear accelerator stayed in the technical background. However, high frequency radar technology in World War II opened new opportunities in linac development. Alvarez, of Berkeley, was the first to build a 200 MHz RF structure, 32 MeV linac for protons. The name **Alvarez structure** is synonymous with today's drift tube linac(**DTL**). Because of the availability of the 200 MHz RF power sources from military radar, the linac structure of those days were tailored to this frequency. These linacs are mainly built as an injector to a synchrotron. Because of the mechanical engineering specifications, such as minimum length of a focusing quadrupole inside the drift tubes, the linacs required over a 750 KeV proton beam as input, provided by a Cockcroft-Walton accelerator. The 200 MeV injectors for the Brookhaven AGS and Fermi Lab. Main Ring booster, were entirely of the Alvarez structure. The highest energy proton linac built to date is an 800 MeV linac, formerly called LAMPF and presently is a part of the LANSCE facility at Los Alamos National Laboratory. The first 100 MeV section of this accelerator is a 200 MHz Alvarez structure, however the rest of the higher energy part is a higher frequency side coupled (cavity coupled) 800 MHz structure(**CCL**).

Several important developments happened in the 1970's. One was the development of permanent magnet quadrupoles and the the second the invention of the radio-frequency quadrupole(**RFQ**) accelerator[15]. One can now build permanent magnet quadrupoles in the field range required for the low energy drift tube. They are physically much smaller than the electromagnet version. Now one can afford to make the drift tube smaller and shorter and thus make it possible to build a higher frequency linac structure for a given pre-injector energy.Thus a linac can be smaller and shorter for a given energy. The radio-frequency quadrupole accelerator suggested by Kapchinski and Teplyakov[15] in 1970 combines focusing and acceleration with the same RF field, and there is no significant limitation on a minimum velocity of the injected beam. The RFQ which replaces the Cockcroft-Walton can accelerate protons from ion source energy of tens of kilovolts to several MeV. A pre-injector is no longer limited to 750 KeV but to many MeV. The linac structures proposed for future accelerators are

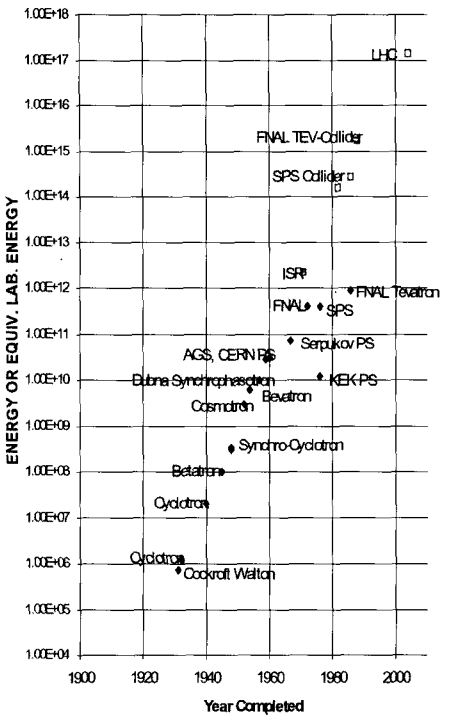

Fig. 1. Simplified Livingston Chart for Proton Accelerators

300 to 400 MHz in the low energy DTL section and are over 700 MHz in the high energy CCL section. The higher frequency structure make it possible to build higher voltage gradient

1.2 Intensity Development

As mentioned, accelerators are mainly developed for the high energy physics experiment. Since there is limit to the proton energy, physicists looking into alternate way to pursuit the ultimate goal. According to uncertainty principle $\Delta E . \Delta t \sim h$ meaning large energy could be replaced by shorter time interval. Other words, very high energy phenomena could be studied by an extremely rear events. In order to generate rear events one needs very high intensity incident protons.

In order to study the rare processes, better detectors and higher and higher intensity accelerators are required. The first problem they encountered was the space charge. The space charge limit is beam intensity limit due to the beam charge distribution because of the repelling force between same electric charges. The problem is worst at the injection energy in synchrotrons. Because of the repulsive force of space charge, the periodic transverse motion of the protons is changed and we call that the space charge tune shift .The space charge tune shift in a given phase space, is proportional to $\beta^2\gamma^3$ (β=v/c, and γ=E/m) and have steep dependence of the proton energy. This led one to look for a higher injection energy. In late 1960's the AGS increased the injector linac energy from 50 to 200 MeV, and the CERN PS increased injection energy by building the 1 GeV booster synchrotron between the linac and the PS. Later the AGS too constructed the booster synchrotron. The idea of booster synchrotron comes from the fact that the space charge tune shift is independent of the size or circumference of the synchrotron in first order. A smaller rings may have higher linear charge density but shorter revolution time relieves them from larger tune shift. The size of the AGS booster is ¼ of the AGS and thus one can expect four times of the intensity in the AGS.

Another hurdle accelerator physicist has to overcome is how to inject high intensity protons into a synchrotron. The usual process was to inject through a thin septum magnet with a collapsing orbit bump to inject many turns from high intensity linac current. It was very inefficient and accompanied with large loss. There was a limit to how high a linac current one can accelerate.

The development of the high intensity H- ion source [16], where a additional electron is attached to the hydrogen atom instead of stripping the electron, and its acceleration was the biggest contributor of synchrotron intensity gains in the early 1970's. According to the Liouville's theorem, for a reversible process one can not inject into a phase space location which is already occupied by another proton. This limits the number of turns one can inject into a synchrotron. However, the theorem only applies to reversible processes. The H- charge exchange process, where two electrons are stripped by a thin carbon foil, is an irreversible process, and the theorem does not apply. One can continue injecting the linac beam in to the same phase space, and pile the protons in to a given phase space volume until stopped by space charge effects or other instability limits. For direct proton injection, the brightness of the linac beam and the thickness of the injection septum magnet limit the phase space density one can inject into a synchrotron. Once the protons are injected into the synchrotron, one has to control the stop bands, resonance bands that cause beam loss and instabilities. A great deal of the work has been done in this area during the last decades.

Another development is the scheme to deal with the transition energy. One of the initial concerns about the viability of strong focusing synchrotrons was the transition problem. In a synchrotron, because of the relativistic effect, the higher energy particle has the higher revolution frequency below the transition energy, and the lower revolution frequency above the transition energy. Transition is the point where particles of all energy have the same revolution frequency. Thus there is no longitudinal phase stability at the transition point. One has to jump the accelerating phase of the RF at a precise moment of the transition. The transition gamma jump system makes the transition crossing easier. There are new lattice designs, which avoid transition or lattices with imaginary transition[17], however there is

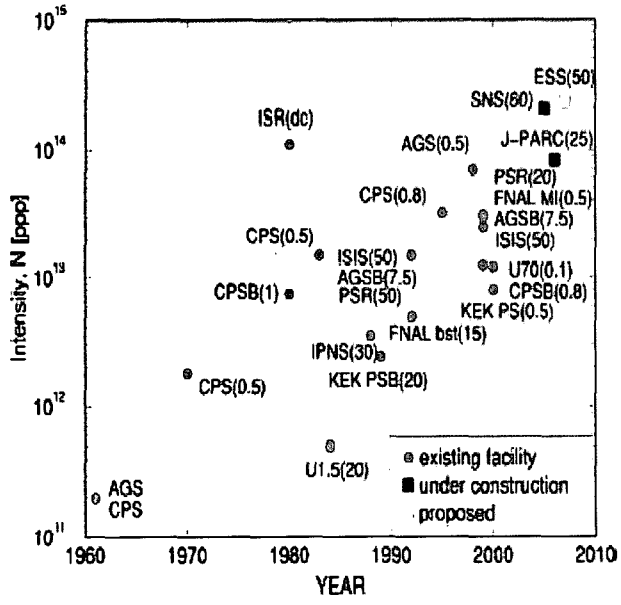

Fig. 2. Evolution of Proton-Beam Intensity (particles per cycle) in Some Synchrotrons and Accumulator/Storage Rings. The Parentheses Indicate Repetition Rate in Hz

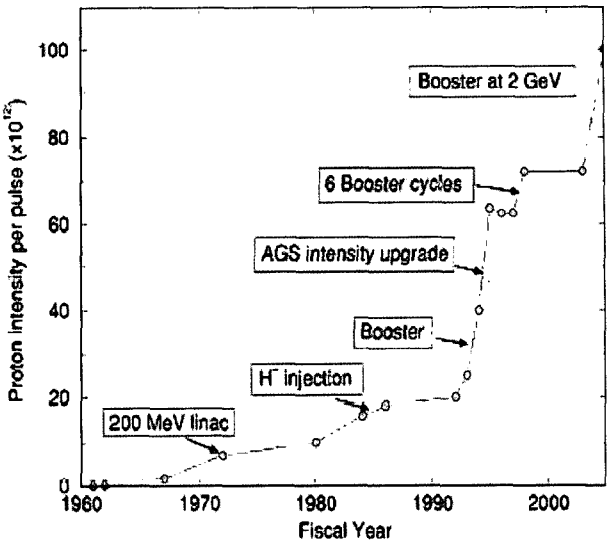

Fig. 3. Evolution of Proton Beam Intensity (particles per pulse) in the Alternating Gradient Synchrotron at the Brookhaven National Laboratory

no such synchrotron constructed to date. The JPARK is first such a synchrotron under construction. The figure 2 shows evolution of the intensity per cycle for typical synchrotrons and accumulator/storage rings including some proposed ones. Development history of the AGS intensity from 10^{10} protons per pulse to the present intensity is a good example.

To illustrate the continuous effort towards attaining high-intensity beams, Fig. 2 shows the evolution of proton intensity in the Alternating Gradient Synchrotron at the Brookhaven. A major increase in intensity was achieved when the injection energy was increased by upgrading the linear accelerator (linac) from 50 to 200 MeV, H- injection replaced proton injection, the AGS booster was constructed to raise the injection energy, the rf is modified so that up to six booster pulses were transferred to a single AGS pulse, nonlinear resonances were corrected in the booster, and feedback systems and dilution cavities were installed in the AGS to suppress instabilities

1.3 Accelerator as a Neutron Source

Traditionally the major source of epithermal to thermal neutrons has been nuclear reactors. They have been excellent continuous sources of neutrons. Although higher power reactors are needed, it has became next to impossible to construct any new reactor in today's political climate. The desire to have intense pulsed sources where the wavelength of the interacting neutrons is measured by time-of-flight has led neutron scientists to propose the use of a proton synchrotron as a spallation source. There are several pulsed

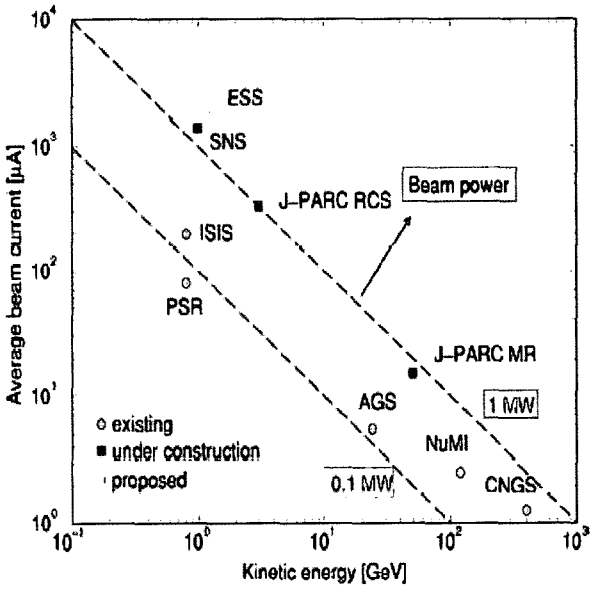

Fig. 4. Beam energy, current, and power of some of the world's high-intensity proton synchrotrons. Beam power in existing high-intensity rings is near 0.1 MW. Beam power designed for new-generation facilities is near 1 MW

neutron sources operating in the world, IPNS at Argonne, ISIS at Rutherford, KENS at KEK, and PSR at Los Alamos.

The proton energy range required for a spallation source is flexible. There have been many proposals to build accelerator based neutron sources. Virtually every accelerator laboratory in the world has proposed a machine over a wide

Table 2. List of Accelerator Based Neutron Source

Laboratory	Devise	Type	Energy (Ring/Linac)	Pulse width	Rep. Rate	Current	Power
Argonne, USA	IPNS	RCS	450/50 MeV	<μsec.	30	15 μA	6.8 KW
Ratherford, UK	ISIS	RCS	800/70 MeV	<μsec.	50	200 μA	160 KW
KEK, Japan	KENS	RCS	500/40 MeV	<μsec.	20	4.6 μA	2.3 KW
Los Alamos USA	PSR	SR	800/800 MeV	<μsec.	20	70 μA	56 KW
Los Alamos USA	LANCE	Linac	800 MeV	1 msec.	60	1.25 μA	1 MW
PSI, Switzerland	SINQ	Cyclotron	590 MeV	CW	CW	1.5 μA	885 KW
KEK, Japan[21]	JPARK Booster	RCS	3 GeV/200 MeV	<μsec.	25	200 μA	600 KW
Oak Ridge, USA	SNS	SR	1/1 GeV	<μsec.	60	1 μA	1 MW*
Europe	ESS	SR	1.334/1.334 GeV	<μsec.	50	3.75 μA	5 MW**
BNL, USA	AGS	SCS	28 GeV/200 MeV	2.7 μsec.	0.6	6 μA	140 KW

RCS; Rapid cycling synchrotron, SR; Storage ring, SCS; Slow cycling synchrotron.
*Upgrade to 2 MW. **consists of two rings.

range of proton energy. Only a few projects are going to be realized. Table II lists the accelerator based neutron sources presently operating. Also included are the SNS[18] which is under construction and to be completed 2006, and the ESS[19]. The JPARK booster synchrotron is under construction. Also included in the table is the AGS, which is the highest intensity per pulse synchrotron with very low repetition rate as comparison. And The figure 4 show the graphically The repetition rate is one of the important factors one has to consider for planning a high power synchrotron complex. The limitations of the power generated by a spallation sources arise from the beam current limitations of the injector linac and the rapid cycling synchrotron or the storage ring.

2. ISSUES

The primary concern in designing high-intensity proton facilities is that radioactivation caused by uncontrolled beam loss can limit a machine's availability and maintainability. Based on past operational experience, hands-on maintenance (1–2 mSv/h or 100–200 mrem/h at 30 cm from the surface, 4 h after shutdown) demands an average uncontrolled beam loss not exceeding about one watt of beam power per tunnel meter [20, 21]. For example, for a ring of 200-m circumference handling a 2-MW beam power, this corresponds to a fractional uncontrolled beam loss of 10^{-4}. Existing proton synchrotrons have beam losses as high as several tens of percent, mostly occurring when the beam is injected, during its initial capture by the accelerating system, at the start of acceleration ramping where the space charge effect is most severe. The best injection loss has been achieved at PSR accumulator ring at Los Alamos of 0.3%, however for accelerating synchrotron, lowest loss achieved is close to 10% because of the capture and initial ramping of the magnetic field. Although a linac is much more expensive to build and less reliable than rapid cycling synchrotrons, the above mentioned problems leads one to choose a full energy linac and an accumulator storage ring for multi-megawatt spallation sources like the ESS and SNS. The debate will continue, however, over the choice of an accumulator storage ring or a rapid cycling synchrotron until the SNS and JPARK booster get completed and operated.

2.1 Injection

As mentioned, the losses at the injection is a significant fraction of the uncontrolled beam loss, and a special attention is needed for the process. Although H^- charge exchange injection is versatile and gives a flexibility of painting phase space, one has to deal with a losses. Injection losses can be in many different processes.

a) Stripping foil multiple and nuclear scattering

As circulating protons traverse through the stripping foil they will scatter and causes a beam loss and emittance growth and/or generate beam halo. Therefore the stripping foil should be as thin as practical though thicker foil for high stripping inefficiency causes another kind of uncontrolled loss. The injection painting scheme should minimize the number of circulating traversal through the foil. The SNS injection has 1000 turns and average foil traversal is about 7. The size of the foil also should be as small as practical to minimize the foil hits.

As ions go through the stripping foil they will heat the foil area. Together with two stripped electron of incoming H^- will deposit 3 times of energy than that of circulating proton hit. The foil heating and cooling will limit the life of the stripping foil. The foil life is a major concern at the accumulator ring like the SNS. A noble method to use a laser power to strip the electron has been proposed and

being developed.

b) Loss due to stripper foil inefficiency

When H^- ions go through a stripping foil, most of the ions lose both electrons and turn into protons. However up to few percent of them would emerge as neutral hydrogen or H^- ion. At the SNS, up to 10% of the ions are expected to emerge non-proton depending on the size and thickness of the stripping foil. Emerging H^- can be safely dumped in predetermined injection dump. The problem is that most of the inefficiency is emerge as a form of neutral hydrogen. The neutral hydrogen will be in various quantum state and each of these quantum state will be further split in to many different Stark states in a magnetic field. The figure 5 shows the life time of each state before Lorentz stripped into a proton for 1GeV SNS injection.

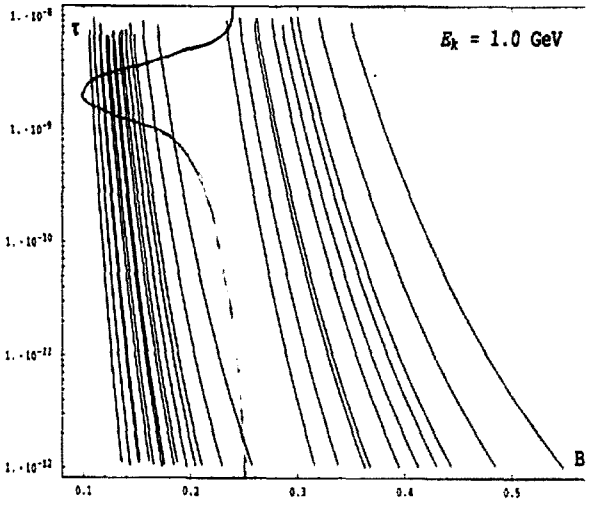

Fig. 5. Stark State Life Time for the SNS Injection. Shown are Principal Quantum State n=4 and 5. Also Shown is the Expected Path of the Hydrogen States in the Injection Chicane of the SNS

The Stark state which stripes immediately($<10^{-11}$ sec.) or survive long enough to pass through the magnetic fields($>10^{-8}$ sec.) does not cause any problem. However, the states which stripes to proton in a phase space of halo or lose at ring elements down stream should be avoided. The hand drawn line in the figure 5 is the expected path the SNS injection. The magnetic field chosen is situated between principal quantum number n=4 and n=5.

The stripping foil is placed between two dipole magnets of which upstream magnetic field of 3 K-gauss is higher than downstream one of 2.4 K-gauss. The placement of the foil is at 2.5 K-gauss point of the descending fringe field downstream of upstream magnet. Expected uncontrolled stripping is order of 10^{-6}.

c) Stripped electron dumping

The power contained in the two electrons of H^- ions are 1000th of the incoming linac power and is 2KW at the SNS. Its emittance is similar to the linac. Unless they are dumped properly, it can cause serious damage to the equipments. So far, for presently operating synchrotron or storage rings, the power is not high enough to damage the vacuum chamber but left unmistakable burn mark at AGS Booster and at PSR. At the SNS the magnetic field around the stripping foil is carefully shaped to guide the electrons to the bottom of the vacuum chamber(fig. 6). The electron catcher is shaped so that stripped electron always strike at the bottom part of the saw tooth shape to prevent any secondary electrons escape inside the aperture volume

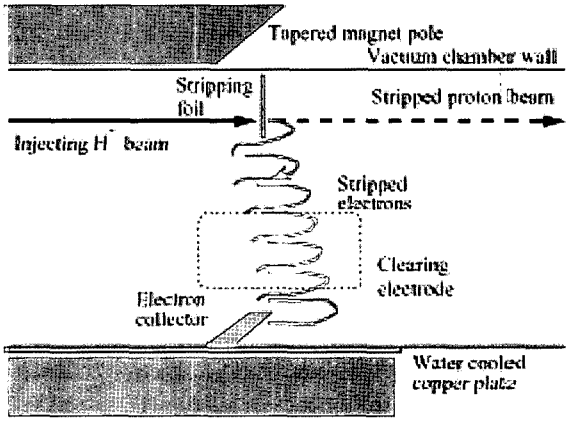

Fig. 6. Collection of Stripped Electrons During the Injection of the H^- Beam at the SNS Ring. The Foil is Placed in a Dipole Magnet, which is Part of the Injection Bump. The Lower Pole Surface of the Magnet is Extended Downstream by about 20 cm so that the Electrons are Guided Down to the Electron Collector

d) Transverse phase space painting

Transverse painting alleviates the fundamental limit on space charge and controls the uniformity and shape of the beam's profile. Transverse phase space distribution of the protons is carefully controlled at the injection process. By carefully programming injection orbit bumps or injection line optics one may control the distribution. The good linac emittance is essential in this process like a good brush is need for good painting. There are two distinct ways to paint the transverse phase space.

Anti-correlated painting utilizes both the horizontal and vertical orbit bumps, one with increasing and the other with decreasing closed-orbit bump amplitude, respectively. Ideally, this painting scheme produces a distribution with an elliptical transverse profile and a uniform density distribution. Many accelerator theorists prefer the scheme. Such a configuration can also be obtained by painting in one direction and steering in the other.(Fig. 7) However, in the presence of strong space charge, this scheme can produce

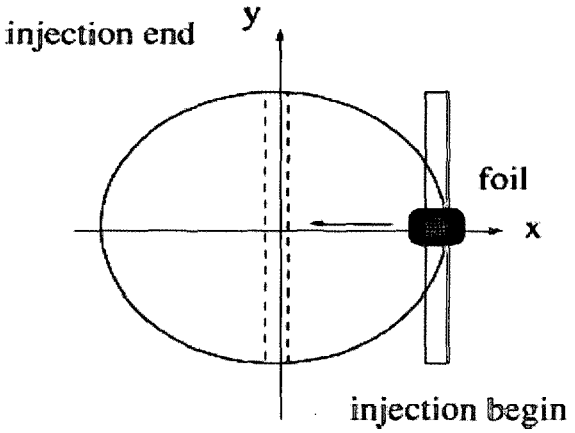

Fig. 7. Beam Transverse Profile of Horizontal Orbit Bump/Vertical Steering Anti-Correlated Painting Similar to the Scheme Used in the Charge-Exchange Injection in the J-PARC 3-GeV Ring

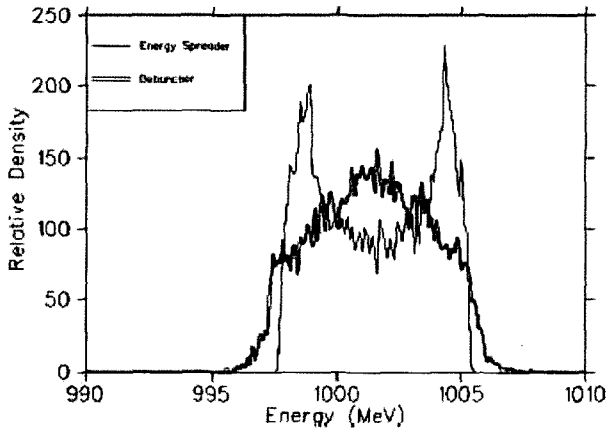

Fig. 9. Energy Distribution at the Injection Foil, Using Either an Energy Spreader or a Conventional Debuncher. An Energy Spreader Significantly Suppresses the Beam Tail.

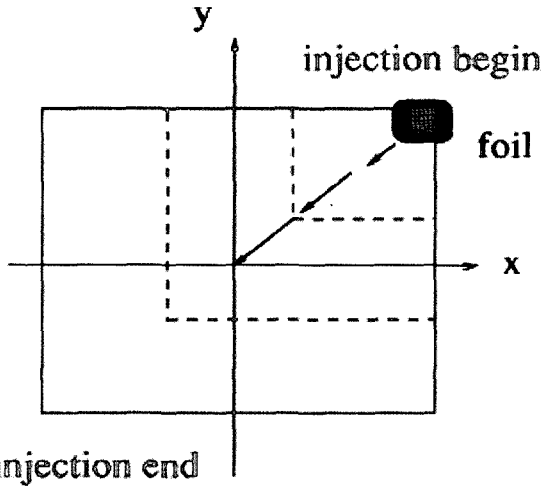

Fig. 8. Beam Transverse Profile of Correlated Bump Painting Used in Charge-Exchange Injection Into the SNS Ring

an excessive beam halo in the direction of the large initial oscillation amplitude, which requires extra clearance.

Correlated painting using same sign horizontal and vertical orbit bumps generates a rectangular transverse profile. Its advantage is that the beam halo is constantly painted over by the freshly injected beam. The main concern is whether the rectangular beam profile can be preserved in the presence of coupling produced by space charge and magnetic guide field. The SNS adopts correlated painting to realize equal transverse emittances, operating near coupling resonance to achieve a fully coupled, circular distribution in the physical dimension.

e) Longitudinal phase space painting

Longitudinal painting provides the momentum spread required for beam stability as well as controlling line density. At the SNS scheme to introduce adequate momentum spread without introducing an excessive momentum halo (Fig. 9). With dispersion-free injection, longitudinal painting can be achieved for linac to ring injection by using an "energy spreader" rf cavity located in the transport line upstream of the injection region, which is phase modulated with respect to the linac frequency. This achieved by running the cavity frequency differ by 100 KHz from the linac frequency and the energy will be modulated by the beat frequency between the cavity and linac. To facilitate such a painting scheme, the injecting beam's momentum jitter and spread need to be controlled, possibly by an "energy corrector" rf cavity synchronized to the linac's frequency, again located in the transport line upstream of the spreader cavity and at an optimized distance from the end of linac [24]. The corrector cavity corrects the energy jitter and spread using phase slippage of off momentum beam. SNS uses this arrangement to allow for adequate beam phase slippage and thus moderate rf voltage. Together with the programmed chopping of the linac beam, one can paint uniform phase space. One also can shape the tail shape of the bunch to minimize multipacting effect of oscillating electron to prevent so called e-P instabilities.

2.2 Acceleration

For synchrotrons, especially for rapid-cycling synchrotrons, significant beam loss often occurs during the injection period when a coasting beam is adiabatically captured by the radio frequency system, and also during initial acceleration when the phase-space area of stable longitudinal motion tends to decrease with the rising synchronous phase. The length(phase axis) of the bunch shortens and linear charge density increases. It causes space charge tune shift to increase considerably even to some beam loss may occur.

The voltage amplitude of the ring rf system must be programmed according to the rising synchronous phase to ensure a increasing rf bucket area. One can flatten the peak beam density in several ways. Radio-frequency systems operating at multiple frequencies can be combined to shape the rf bucket. For example a dual-harmonic system, the frequency of the secondary rf system is chosen to be an integral multiple of the fundamental rf system. Typically the ratio in operating voltage amplitude is inversely proportional to the ratio in rf frequency. With this choice, the frequency of synchrotron oscillation extends from zero at the center of the bucket to a maximum value across its core about 1.2 times the maximum synchrotron frequency of a single harmonic system [25,26]. Thus the spread of synchrotron frequency in the bunch usually is greatly enhanced.

The magnet power supply and rf systems represent major engineering challenges associated with fast energy ramping. At present, three types of magnet power system commonly are used for synchrotrons: bridge rectifiers directly connected to the power grid (AGS Booster, FNAL main ring); bridge rectifiers with local energy storage in the motor generator set (AGS, CERN PS); and, resonant power systems with local energy storage in capacitors and chokes (ANL IPNS, Rutherford ISIS). Rapid-cycling synchrotrons demand a large amount of reactive electrical power (typically tens of megawatts) for the magnet. While it is flexible on magnetic cycle and easy to accommodate multiple users. a direct powering has its problems. A large amount of reactive power is swishing back and forth in the power grid and careful choice of compensation and operating repetition rate. Otherwise, entire power grid may suffer voltage oscillation. A local energy storage system like a large motor generator is also flexible without interacting with the power grid system, but it is expensive to implement and operate. The higher the repetition rate, the larger is the peak power exchanged with the power grid or motor-generator, and the more likely is the need for large local energy storage. Thus most existing rapid cycling synchrotrons use resonant power systems. With a resonant power system, the strength of the magnetic field varies sinusoidally along with the rigidity of the beam. The consequences are the lack of a "flat bottom" for a static injection condition, and the demand for high voltage amplitude by the rf system to sustain the largest ramping slope of the sinusoidal wave form. The quality of the magnet field usually suffers from current-induced effects and saturation. In order to alleviate the large rf demand, a multi-harmonic ramping with a slower slope during the up ramp (acceleration) and faster slope during the down ramp had been proposed[27,28]. But no such a system is successfully implemented yet to date. To satisfy the increasing need to accurately control the injection "flat bottom" and extraction "flat top," and to have a flexible program of magnet current, high frequency ac bridge rectifier systems are under development, such as those based on IGBT (insulated gate bipolar transistor) rectifiers. A programmable ramp using this technology provides maximum flexibility in manipulating the profile of the rise and fall, thus reducing the peak ramp rate and current-induced magnetic imperfections. with beam dynamics, accelerator control, and diagnostics. On the other hand, in comparison with colliders where the beam is stored for an extended period of time, requirements on power supply ripples and rf system noise for a typical high power ring are less stringent due to the relatively short time period of beam accumulation and acceleration.

Radio frequency system(rf) for proton acceleration is generally consists of ferrite loaded rf cavity. Frequency is controlled by inductance change as the ferrite saturates. The rf voltage achievable for this kind of cavity is limited by the losses in the ferrite and about 10 KV per meter of straight section. The ferrite has to be cooled in order to keep the magnetic property of the ferrite stable. A new kind of material to be used for this kind of cavity is being developed. A typical example is the crystalline magnetic alloys like Finemet. Finemet have successfully achieved a gradient of 50 kV/m at the AGS. The material is stable for wide range of temperature, however rf losses are much more than typical ferrite thus require more rf power. The engineering feat is how to cool the material. JPARK project is planning to use this material extensively.

Radio-frequency "beam loading" refers to the transient response of the rf system to variations in the beam's current, frequency, and energy. Compensation for "beam loading" aims at maintaining a stable accelerating voltage in the presence of varying beam conditions. The effect of beam loading is simpler at accumulator ring where the energy and the frequency is fixed. New challenges are associated with compensating high-intensity beam loading in the magnetic alloy cavities where the Q is very low and broadband resonance spans several rf harmonic frequencies. Detailed engineering design is needed to minimize system noises. Measures like ground break (separation of electrical grounding of different accelerator systems) are used to isolate pulsed signals from high-power power-supply systems and to minimize their interference with beam dynamics, accelerator control, and diagnostics.

2.3 Beam Loss Mechanism and Collimation

Beam loss is categorized into two classes: controlled and uncontrolled. Controlled beam loss generally is losses reaching the beam dump and absorbed at the collimators, both located in shielded regions. The controlled losses include the beam's tail from the linac H- beam missing or escaping the stripping-foil reaching the injection beam dump The beam halo generated in the ring, energy straggling at the foil, and loss due to the kicker's misfiring are typical source of the uncontrolled loses The beam dump and collimators must withstand the effects of the beam's high power, power density, and repetition rate. Mechanical analyses with computer simulation programs like ANSYS and performance tests of prototypes are essential, including

their resistance to thermal, radiation, and mechanical stresses, vacuum out gassing, vacuum leakage, and long-term fatigue An example is the window to the beam dumps that separates the accelerator vacuum from the atmosphere.

The beam halo generated in the ring can be cleaned both in the transverse and the longitudinal phase space in controlled fashion. For transverse collimation, scrapers and collimators are arranged in dispersion-free regions. Optimization of the relative phase advance and the acceptance of the primary scraper and secondary collimators maximizes the efficiency of collimation and minimizes beam loss on unprotected elements .Efficient collimation requires an adequate acceptance ratio between the scraper and collimators, and the rest of the vacuum pipe. Longitudinal phase space cleaning can be accomplished in the momentum and in the azimuthal phase. The momentum halo can be cleaned by scraping at a high-dispersion lattice location or using a beam in gap kicker The latter method requires an adequate momentum clearance so that particles can reach the gap without loss. Azimuthal phase cleaning, or cleaning of the "beam gap," can be done with a wideband beam kicker in lock step with the beam tune.

Primary scrapers are usually adjustable, thin blades, the material and thickness of which are optimized for scattering, heating, and other engineering properties. The primary scraper of the SNS ring consists of four tantalum blades, each 5 mm thick. They are spaced in 45° angles, adjustable to the varying needs of collimation aperture. The scraper assembly is shielded for containing radioactivity. Secondary collimator and collector units designed for high-intensity synchrotrons typically are nonadjustable, complex elements, unlike collimators meant for high energy experiments that often consist of adjustable solid metal jaws. Anticipating a relatively high beam power to be scraped, these units are cooled by closed loop circulating water in order to avoid mixing of the radioactive water to rest of the system. The function of these unit is to contain good fraction(typically over 90%) of secondary charged and neutral particles as well as to stop the primary beam. Figure 10 shows the collimator design for the SNS accumulator ring. The vacuum chamber is made of double-layered stainless steel filled with helium gas between the layers to detect leaks. Due to stringent engineering requirements for stress and heat tolerance, thermal contraction, and shielding, for operational reliability these units are not adjustable in collimation cross section. The secondary particles escaping the collimator system are main component of the uncontrolled beam losses. Rest of the uncontrolled loss is due to the proton reaching vacuum chambers without being intercepted by the scraper. The aperture ratio of scraper to the rest of the vacuum chamber is important in controlling the loss.

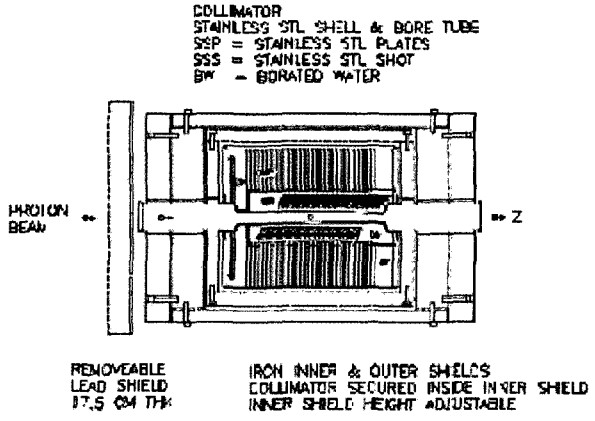

Fig. 10. Schematics of One of the SNS Ring's Secondary Collimators, Showing Layers of Material for Radio-Activation Containment. The Effective Length is About 1.5 m. The Collimator is Designed to Withstand an Average Beam Power of up to 10 kW at 1 GeV Kinetic Energy

2.4 Collective Effects

Collective effects limit the beam current in a high-intensity synchrotron system. Collective effects can arise either directly from electromagnetic interaction of particles in the same bunch (space-charge effect) or indirectly through other media. Since a particle beam generates an electromagnetic field while passing through discontinuities and variations in the vacuum chamber's cross-sectional shape and conducting properties it can induce a signal to the chamber. The effects of Coulomb scattering among particles of the same bunch (intra-beam scattering) usually is negligible during the short time of accumulation and acceleration.

a) Space Charge Effects

Space-charge effects set a fundamental limitation for high-intensity synchrotrons. In contrast to linacs, where longitudinal and transverse bunch sizes are similar, in proton synchrotrons the longitudinal size of the bunch is usually much longer than its transverse dimensions. Accordingly, transverse space-charge tune shifts are orders of magnitude larger than the longitudinal ones, and longitudinal and transverse space charge usually can be considered separately. In the longitudinal direction, space charge contributes a defocusing force below the transition energy. The longitudinal spread of the bunch may cause particles to escape from the rf bucket, requiring compensation by enhancing rf field focusing or introducing an inductive impedance into the ring [29]. In the transverse direction, the dominant effects are the coupling of the transverse motions and the development of space charge resonances. The coherent tune of the beam, along with the associated collective oscillations, determines its resonant behavior. To prevent significant beam broadening and emittance growth, it is

necessary to maintain the coherent tunes of the beam away from low order imperfection and structure resonances. The choice of working tune is based on a consideration of the space charge resonances and avoidance of higher order resonances excited by lattice nonlinearity in the presence of space charge-induced tune spread. When the horizontal and vertical tunes are close to each other, significant exchange of emittance also occurs, generating a round beam in the transverse physical space On the other hand, beam core parametric resonance induced by beam mismatch, which is the primary source of halos in a proton linac, often is unimportant, especially for a multi-turn injected ring when the halo is covered by the subsequently injected beam. The most effective approach to resolving space charge problems is to raise the injection energy. Space charge can also be alleviated by longitudinal manipulation like duel harmonic rf cavity to manipulate the bunching factor, and by transverse and longitudinal painting and controlled injection as discussed at injection section. Longitudinal space-charge compensation using inductive inserts to counter the capacitive effect of the space charge has also been demonstrated at the PSR in Los Alamos.

b) Coupling Impedances

The coupling impedance describes the interaction between a beam and its environment It is the ability to exchange information between the beam current and its environment like vacuum chamber, pick up electrode and other diagnostic devices, injection or extraction equipments and rf cavities to name a few. It can cause a beam instability and beam losses. [29, 30] It is divided into two components, longitudinal and transverse and both are complex quantities of imaginary and real. The longitudinal impedance usually is quantified as Z/n where n is mode number and multiple of the rotation frequency. The vertical and horizontal coupling impedances are defined as the integrals of the deflecting fields over one turn, normalized by the dipole moment of the excitation beam current and quantified as Z/m where m is offset from the center in meters. The effect is on the off axis beam Minimizing the impedance is an important measure to prevent collective instabilities. Any discontinuity in the vacuum chamber can act as a rf cavity and enhances impedances, thus the smoothness of the chamber is essential to minimize impedances. Below transition energy, the reactive or imaginary part of the impedance generally is dominated by space charge. Both transverse and longitudinal space charge impedances can be reduced by allowing the contours of the conducting vacuum enclosure to follow the variations in the beam's envelope. A example of this is at the ISIS synchrotron, using metal wires contoured to the beam's envelope inside the ceramic beam pipe [31].

The growth of an instability is associated mostly with the resistive(real) part of the transverse impedance. For the ISIS synchrotron, as well as the SNS and the ESS accumulator ring, the leading resistive component of the coupling impedance is from the extraction kicker modules located in the vacuum chamber. The coupling impedance is minimized by the design of the pulse forming network (PFN) power supply circuits (low termination impedance). The frequency dependence of the coupling impedance further depends on the permeability of the ferrite material. Ferrite material of relatively low permeability and low resistive loss was found to be beneficial if the PFN was not terminated with a low impedance [32] Impedance due to the resistive wall of the vacuum chamber can become important at low frequencies. Investigations have been pursued on the coupling impedance of thin resistive layers, such as the metallic coatings of ceramic vacuum chambers in kicker magnets. Theoretical studies showed that the beam's image current flows in the resistive layers, even in the low frequency regime when the layers are much thinner than the skin depth, unless external structures offer alternative paths of lower impedance. At very low frequencies, where square of the skin depth exceeds the product of the chamber's radius times the layer's thickness, a significant reduction in the real part of the transverse impedance might be expected. These predictions were validated by preliminary bench measurements at CERN [33, 34]. Two layers of coating were applied to the SNS ring's ceramic chamber for injection kickers: a 1 mm-thick copper layer for by passing the image charge and a 0.1- mm-thick titanium nitride (TiN) layer for a low secondary electron yield, along with an exterior metal enclosure for dc current bypass. Such a design allows the passage of the image current above a frequency of the lowest betatron sideband (;200 kHz) without degrading the magnetic-field penetration (a rise time of about 200 μs), eddy-current heating, and beam induced heating. Improvements to the vacuum chamber bypass also are planned at the CERN PS Booster, and shielding of the magnet septa and vacuum ports is underway at the CERN SPS. LANL (PSR) and KEK assessed the ability of inductive inserts to compensate for the longitudinal space-charge coupling impedance. Such devices are considered practical for machines like the proposed CERN accumulator, which requires an inductive Z_i / n of 70 Ω, with a real part no larger than 1 Ω [21]. Computer modeling frequently is used to predict the coupling impedance of a device [35]. However, computation becomes inefficient when the geometry of the device is complex and asymmetric and when the material's permeability is high. Bench measurements are needed to determine the impedance of critical devices, e.g., the extraction kicker and its power-supply (PFN) network [36, 37, 32]. After the machine is constructed, the total coupling impedance can be determined by measuring the beam's transfer function, energy loss, and tune shifts [30]

c) Instabilities

Instabilities are common in proton rings [32,38,39]. Due to the short accumulation time (typically around one

synchrotron oscillation period), a proton beam in an accumulator is susceptible only to fast, transverse instabilities like the electron-proton instability which limits the beam intensity in the PSR ring [40]. However, rapid-cycling and conventional synchrotrons are susceptible to an extended list of instabilities. Head-tail instabilities were observed near injection in the KEK PS, the CERN PS, and the AGS and are suspected to be due to chromaticity change caused by eddy current induced sextupole fields in the vacuum chamber in the dipole magnets. This type of instability can be cured by chamber correction windings like the one used in the AGS Booster, chromaticity control, Landau damping with octupoles, and tune manipulation. Negative mass and microwave instabilities are observed at the CERN PS and SPS, the AGS, and the KEK PS. They can be avoided by measures that reduces coupling impedance, and that improve the bunching factor. Instability in coupled bunches was observed at the CERN PS Booster, PS, and SPS, and the AGS and was damped by fast feedback systems and Landau damping systems. The ISIS programs the tunes in each cycle to accommodate natural variations in chromaticity, to depress space-charge and to avoid the resistive wall head tail instability [41].

The observed threshold for longitudinal instability may not correspond to that estimated from the Keil-Schnel criterion[42,43,44,45], especially in the presence of a strong space charge. Examples are the ISIS synchrotron, the CERN PS, and the AGS Booster. In longitudinal direction, space charge typically reduces the growth rate of instability with its debunching force (below transition) and results in selfstabilization [46.47,48,49,50,51]. Transversely, space charge lowers the instability threshold by altering the mode frequency and mode-coupling condition[52,53]. Recent developments in computer simulation have made it possible to investigate the mechanism numerically[54,55]. Longitudinal and transverse coupled bunch instabilities are mostly driven by the parasitic resonances in the rf system. Such instability is often cured by passively damping such resonances or by installing a fast bunch-by-bunch damper. Feedback systems frequently are used to damp instabilities. The long wake of resistive wall impedance may cause a closed-orbit drift during acceleration that can be damped by a slow rate feedback system [56]. However, faster rate feed back systems are required to damp instability like electron cloud instability, and coupled bunch instability.

d) e-P Instability

Electron-cloud effects are important, but not completely understood dynamical phenomena. Effects that can severely limit the performance of high intensity proton synchrotrons include trailing edge tune shift and resonance crossing, electron-proton instability, emittance growth and beam loss, increases in vacuum pres-sure, heating of the vacuum pipe, and interference with beam diagnostics. The following are examples of hadron rings where electron cloud effects had been observed: the Proton Storage Ring (PSR) at the Los Alamos where a strong, fast transverse instability occurs both for coasting and for a bunched beam when a threshold intensity is exceeded [57]. the CERN PS and SPS, where a large number of electrons are produced by beam induced multipacting when the machine's parameters are configured for LHC injection [58,59], and the Relativistic Heavy Ion Collider (RHIC), where the vacuum pressure dramatically increases when the beams are injected with half nominal bunch spacing. Electron-cloud effects could limit the performance of the next-generation high-intensity proton rings, such as the Spallation Neutron Source's (SNS's) accumulator ring, and neutrino-factory proton drivers.

Sources of electrons in ring are: electrons generated at the stripping foil, electrons generated at collimators and vacuum-pipe surfaces by lost protons, electrons produced by multipacting from the vacuum chamber's wall; and, electrons produced around the ring from residual gas ionization. As an example, Fig. 11 shows the distribution of electron-density flux measured at the PSR using the electron detector developed at the Argonne National Laboratory [60]. Beam-induced multipacting is believed to be the leading source of sustained electron production. Depending on the beam parameters, one of two multipacting models applies: multibunch passage multipacting [61,62, 63, 64, 65], or single-bunch, trailing edge multipacting [66, 67] The phenomenon of multi-bunch, beam induced multipacting was observed at the CERN PS and SPS when the machines' parameters were configured for LHC injection. The electron-cloud buildup was sensitive to the intensity, bunch spacing, and length of the proton bunches, and to the secondary emission yield of electrons from the beam pipe surfaces.

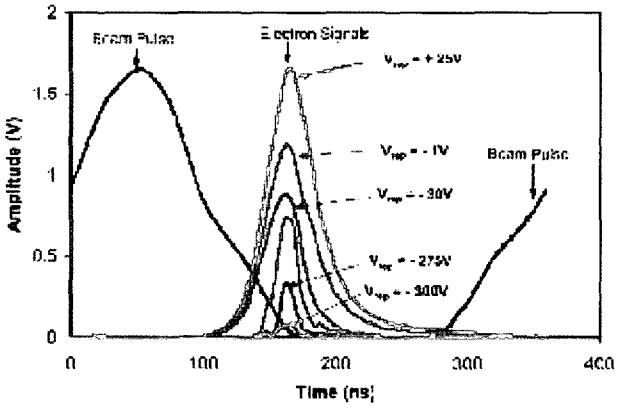

Fig. 11.. Electron Signals Measured at the PSR as a Function of Time Relative to the Proton-Beam Pulse During a Single Revolution. The Proton Bunch Length is About 250 ns. The Repeller Voltage V_{rep} is Varied to Select the Electrons Striking the Detector According to their Energy

The multi-bunch multipacting occurs if the transit time of the electrons crossing the vacuum pipe is same with the time between successive bunches and if the electrons gain enough energy to produce more than one secondary electron when they hit the vacuum pipe wall [62]. This phenomena is similar to the traditional rf multipact depending on the accelerating rf voltage and the electron transit time. This can be alleviated by disrupting the regularity of bunch spacing.

Single bunch, trailing-edge multipacting starts to dominate if the bunch length is long enough to sustain multiple passes of electrons in its trailing edge. At the trailing edge of the proton bunch, electrons are accelerated and released by slightly lower potential because of the longitudinal bunch shape distribution. The difference of potential gives the electron enough energy to produce secondary electrons. In Los Alamos PSR case the electron makes tens of passes. The number of electrons grows dramatically at the trailing edge of the proton bunch, as observed at the PSR (Fig. 11) [68]. The electron-cloud buildup due to this single-bunch mechanism is expected to have a weak or no dependence on bunch spacing, the vacuum pressure level, and the amount of residual protons in the beam gap. However, it depends critically on the length of the proton bunch and the variations in its longitudinal density. Various computer simulation programs were developed to model the process of electron generation [69,63,64]. Simulations included space charge fields of both protons and electrons, vacuum pipe and image charges, external magnetic fields, gas ionization, secondary emission, and photo-emission. Recent developments have incorporated trailing edge multipacting, rediffusion, backscattering, and proton induced secondary emission with refined angular dependence of the incident particle [70,71,72]. Particle-in-cell (PIC) algorithms also were developed to model detailed electron-generation processes [73]. An electron cloud tends to neutralize the positive charge of the proton beam. Compared to the space-charge tune shift between the protons, the tune shift produced by an electron cloud is enhanced by a factor γ^2 due to absence of compensating electric and magnetic forces in the laboratory frame. With the trailing-edge electron multipacting model, protons at the trailing edge of the bunch experience, on average, a high concentration of electrons. Electron neutralization increases the transverse tunes and possibly increases the tune shift of the beam. When the beam is stored in the ring for an extended time, the bunch may continuously lose its trailing edge particles upon resonance crossing. We refer to this as the trailing edge Pacman effect. Remedy for this is to prevent or minimize the electron multiplication in the trailing edge. Longitudinal painting can be effective way to minimize the number of electron traversals. The vacuum chambers can be coated with TiN to minimize secondary emission coefficient. And also reduce the source of electron inside the ring. Longitudinal painting to control the momentum spread in the ring to enhance Landau damping could be effective.

3. DISCUSSIONS

So far synchrotrons and accumulators have advanced to meet the challenge of the next generation applications. Difficulties encountered in progress demand state of the art knowledge and technology from the physics community and the industry. Accelerator physics and technologies developed at the high intensity frontier in turn stimulate the evolution of modern accelerators.

A key challenge in achieving a high-intensity performance is to minimize uncontrolled beam loss. Beam losses are attributed to single-particle and multi-particle phenomena. Leading single particle phenomena include injection related losses, magnetic nonlinearities, and resonance crossing. Leading multi-particle phenomena include space charge effects, instabilities due to coupling impedances, and electron cloud effects. Rapid cycling synchrotrons have lower injection energy and fewer accumulated particles thus the injection loss problem may be less severe. On the other hand, fixed energy accumulators do not accelerate beam in the ring, and the beam accumulation time is short. In designing a new high intensity synchrotron, question of "Is it preferable to use a rapid cycling synchrotron, or a fixed energy accumulator?" must be answered. What roll the superperiodicity play in the designing of the system? How are injection, rf, collimation, and extraction to be arranged? Answers to these questions are closely related to considerations of beam loss. Above all, having a large transverse vacuum pipe aperture and long, uninterrupted straight sections are the two most important aspects that must be considered from the very beginning.

REFERENCES

[1] Jie Wei, Reviews of Modern Physics, 75(2003) 1383
[2] R. J. Van de Graaf, 'A 1,500,000 volt electrostatic generator' Phys. Rev.,387, 1990-20
[3] J. D. Cockcroft and E. T. S. Walton, 'Experiments with high velocity ions' Proc. Royal Soc., Series A 136(1932), 619-30
[4] G. Ising, Arkiv for Matermatik. Astronomi och Fysik,18, (1924), 1-4
[5] R. Wideroe, Arch. Fur Elektrotechnik, 21(1928),386-406
[6] E. O. Lowrence and N. E. Edlefsen, Science,72(1930) 376-7
[7] See for example P. Waloschek, 'The Infancy of Particle Accelerators' DESY report 94-039(1994)
[8] D. W. Kerst, 'The acceleration of electrons by magnetic induction' Phys. Rev., 60(1941), 47
[9] D. W. Kerst, and R. Serber, 'Electronic orbits in the induction accelerator' Phys. Rev. 60(1941), 53
[10] E. M. McMillan, 'Synchrotron – a proposed high energy accelerator' Phys. Rev. Letter to the editor, 68(1945), 1434
[11] V. Veksler, J. of Phys., USSR, 9(1945), 153
[12] E. D. Courant, M. S. Livingston and H. S. Snyder, 'The strong-focusing synchrotron – a new high energy accelerator' Phys. Rev., 88(1952), 1190

[13] E. D. Courant and H. S. Snyder, 'Theory of alternating-gradient synchrotron' Annals of Physics, No. 3(1958), 1
[14] N. C. Christofilos, Unpublished report(1950)
[15] Kapchinskii, I. M., and V. A. Teplyakov, 1970, Prib. Tekh. Eksp. 119, 19.
[16] Hiskes, J. R., A. Karo, and M. Gardner, 1976, J. Appl. Phys. 47, 3888.
[17] Trbojevic, D., D. Finley, R. Gerig, and S. Holmes, 1990, in*Proceedings of the European Particle Accelerator Conference*, Nice, France, edited by P. Marin and P. Mandrillon (EditionsFrontie` res, Gif-sur-Yvette, France), p. 1536.
[18] SNS conceptual design report(1997) The SNS is approved to be constructed stating oct. (1998).
[19] ESS conceptual design report(1997)
[20] Wangler, T. P., 1998, Principles of RF Linear Accelerators (Wiley, New York).
[21] Chou, W., and J. Wei, 2001, in Proceedings of Snowmass 2001,
[22] Jason, A. J., B. Blind, P. J. Channell, and T.-S. F. Wang, 1994, in Proceedings of the 4th Particle Accelerator Conference, Lon-don,edited by V. P. Suller and Ch. Petit-Jean Genaz (World Scientific, Singapore), p. 1219.
[23] Abell, D., Y. Y. Lee, and W. Meng, 2000, in Proceedings of the 7th European Particle Accelerator Conference, Vienna, edited by J.-L. Laclare *et al.* (Austrian Academy of Science Press,Vienna), p. 2107.
[24] Raparia, D., J. Alessi, Y. Y. Lee, and W. T. Weng, 1998, Brookhaven National Laboratory, Technical note SNS/52.
[25] Hofmann, A., and S. Myers, 1980, in Proceedings of the 11thInternational Conference on High Energy Accelerators, Geneva, edited by W. S. Newman (Birkha¨ user, Basel), p. 610.
[26] Wei, J., 1992, in Proceedings of the 3rd European Particle Ac-celerator Conference, Berlin, edited by H. Henke, Ch. Petit-Jean Genaz, and Homeyer (E ′ ditions Frontie′ res, Gif-sur-Yvette, France), Vol. 1, p. 833.
[27] IPNS, 1995, The IPNS Upgrade (Argonne National Laboratory, Argonne, IL).
[28] FNAL PD, 2000, The Proton Driver Design Study Fermilab -TM-2136 (Fermilab, Batavia, IL).
[29] Sessler, A. M., and V. G. Vaccaro, 1967, CERN Report ISR-RF/67-2.
[30] Zotter, B., and S. Kheifets, 1998, Impedances and Wakes in High-Energy Particle Accelerators (World Scientific, Sin-gapore).
[31] Boardman, B., 1982, Ed., Spallation Neutron Source: Descrip -tionof Accelerator and Target, Rutherford Appleton Labora -tory Report RL 82-006.
[32] Davino, P., H. Hahn, and Y. Y. Lee, 2002, in Proceedings of European Particle Accelerator Conference, Paris, edited by T. Garvey et al. (EPS-IGA and CERN, Geneva), p. 1467.
[33] Piwinski, A., 1977, IEEE Trans. Nucl. Sci. NS-24, 1364.
[34] Caspers, F., et al., 2000, in Proceedings of the 7th European Particle Accelerator Conference, Vienna, edited by J.-L. Laclare et al. (Austrian Academy of Science Press, Vienna), p. 376.
[35] Weiland, T., 1998, in Handbook of Accelerator Physics and En-gineering: A Compilation of Formulae and Data, edited by A. Chao and M. Tigner (World Scientific, Singapore), p. 199.
[36] Nassibian, G., and F. Sacherer, 1979, Nucl. Instrum. Methods 159, 21.
[37] Wang, J. G., and S. Y. Zhang, 2000, in Proceedings of the 7th European Particle Accelerator Conference, Vienna, edited by J.-L. Laclare et al. (Austrian Academy of Science Press, Vi-enna), p. 972.
[38] Neil, V. K., and A. M. Sessler, 1965, Rev. Sci. Instrum. 36, 429.
[39] Chao, A., 1993, Physics of Collective Beam Instabilities in High Energy Accelerators (Wiley, New York).
[40] Macek, R., et al., 2001, in Proceedings of the 2001 Particle Ac-celerator*Conference*, Chicago, edited by P. Lucas and S. Web-ber(IEEE, Piscataway, NJ), p. 688.
[41] Rees, G., 1994, in Proceedings of the 4th European Particle Accelerator Conference, London, edited by V. P. Suller and Ch. Petit-Jean Genaz (World Scientific, Singapore), p. 241.
[42] Nielson, C. E., A. M. Sessler, and K. R. Symon, 1959, in Proceedings of the International Conference on High-Energy Accelerators and Instruments, Geneva, edited by L. Kowarski (CERN, Geneva), p. 239
[43] Ruggiero, A. G., and V. G. Vaccaro, 1968, CERN Report ISR-TH/68-33.
[44] Keil, E., and W. Schnell, 1969, CERN Report TH-RF/69-48.
[45] Boussard, D., 1975, CERN Report Lab II/RF/Int./75-2.
[46] Hofmann, I., 1985, Laser Part. Beams 3,1.
[47] Rumolo, G., I. Hofmann, G. Miano, and U. Oeftiger, 1998, Nucl. Instrum. Methods Phys. Res. A 415, 411.
[48] Hofmann, I., and O. Boine-Frankenheim, 1999, in Workshop on Instabilities of High-Intensity Hadron Beams in Rings, AIP Conf. Proc. No. 496, edited by T. Roser and S. Y. Zhang (AIP, Melville, NY), p. 85.
[49] Koscielniak, S., 1999, in Workshop on Instabilities of High-Intensity Hadron Beams in Rings, AIP Conf. Proc. No. 496, edited by T. Roser and S. Y. Zhang (AIP, Melville, NY), p. 391.
[50] Boine-Frankenheim, O., and I. Hofmann, 2000, Phys. Rev. ST Accel. Beams 3, 104202. NJ), Vol. 3, p. 1723.
[51] Woody, K., J. A. Holmes, V. Danilov, and J. D. Galambos, 2001, in Proceedings of the 2001 Particle Accelerator Conference, Chicago, edited by P. Lucas and S. Webber (IEEE, Piscataway, NJ), Vol. 3, p. 2057.
[52] Blaskiewicz, M., 1998, Phys. Rev. ST Accel. Beams 1, 044201.
[53] Fedotov, A. V., and I. Hofmann, 2002, Phys. Rev. ST Accel. Beams 5, 024202.
[54] Galambos, J. D., J. A. Holmes, D. K. Olsen, A. U. Luccio, and J. Beebe-Wang, 1999
[55] Malitsky, N., et al., 1999, in Proceedings of the 1999 Particle Accelerator Conference, New York, edited by A. Luccio and W. MacKay (IEEE, Piscataway, NJ), Vol. 4, p. 2713.
[56] Danilov, V., S. Henderson, J. A. Holmes, and A. Burov, 2001, Phys. Rev. ST Accel. Beams 4, 120101.
[57] Macek, R., 1999, in Workshop on Two-Stream Instabilities in Accelerators and Storage Ring, Santa Fe, edited by K. Hackay and R. Macek
[58] Arduini, G., et al., 2000, in Proceedings of the 7th European Particle Accelerator Conference, Vienna, edited by J.-L. Laclare et al. (Austrian Academy of Science Press, Vienna), p. 1611.
[59] Me` tral, E., R. Cappi, M. Giovannozzi, G. Me` tral, and F. Zim-mermann, 2001, in Proceedings of the 2001 Particle

Accelera-tor Conference, Chicago, edited by P. Lucas and S. Webber (IEEE, Piscataway, NJ), p. 682.
[60] Rosenberg, S., and K. Harkay, 2000, Nucl. Instrum. Methods Phys. Res. A 453, 507.
[61] Gro¨ bner, A., 1977, in Proceedings of the 1977 International *Conference on High Energy Accelerators*, Protvino, edited by Yu. M. Ado, A. G. Afonin, V. I. Gridasov, A. F. Dunaitsev, E. A. Mjae, and A. A. Naumov (Institute of High Energy Phys-ics, Protvino, USSR), p. 277.
[62] Gro¨ bner, A., 1997, in Proceedings of the 1997 Particle Accel-erator *Conference*, Vancouver, B. C., edited by M. Comyn, M. K. Craddock, M. Reiser, and J. Thomson (IEEE, Piscataway, NJ), p. 3589.
[63] Furman, M. A., and G. R. Lambertson, 1997, KEK Proceed -ings 97-17, edited by Y. H. Chin (KEK, Japan), p. 170.
[64] Zimmermann, R., 1997, LHC Project-Report 95, and SLAC-PUB- 7425.
[65] Ruggiero, F., G. Rumolo, and F. Zimmermann, 2001, Phys. Rev. ST Accel. Beams 4, 012801; 4, 029901(E).
[66] Danilov, V., A. Aleksandrov, J. D. Galambos, D. Jeon, J. A. Holmes, and D. K. Olsen, 1999, in Workshop on Instabilities of High-Intensity Hadron Beams in Rings, AIP Conf. Proc. No. 496, edited by T. Roser and S. Y. Zhang (AIP, Melville, NY), p. 315.
[67] Macek, R., 1999, in Workshop on Two-Stream Instabilities in Accelerators and Storage Ring, Santa Fe, edited by K. Hackay and R. Macek
[68] Macek, R., et al., 2001, in Proceedings of the 2001 Particle Ac-celerator Conference, Chicago, edited by P. Lucas and S. Web-ber (IEEE, Piscataway, NJ), p. 688.
[69] Ohmori, C., et al., 1999, in Proceedings of the 1999 Particle Accelerator Conference, New York, edited by A. Luccio and W. MacKay (IEEE, Piscataway, NJ), Vol. 1, p. 413.
[70] Blaskiewicz, M., 2000, in Proceedings of the 7th European Par-ticle Accelerator Conference, Vienna, edited by J.-L. Laclare et al. (Austrian Academy of Science Press, Vienna), Vol. 4, p.1110.
[71] Danilov, V., A. Aleksandrov, J. Wei, and M. Blaskiewicz, 2001, in Proceedings of the 2001 Particle Accelerator Conference, Chicago, edited by P. Lucas and S. Webber (IEEE, Piscat-away, NJ), Vol. 3, p. 1749.
[72] Pivi, M., 2002, CERN Report CERN-2002-001.
[73] Wang, T. S., P. J. Channell, R. Macek, and R. C. Davidson, 2001, in Proceedings of the 2001 Particle Accelerator Confer-ence, Chicago, edited by P. Lucas and S. Webber (IEEE, Pis-cataway, NJ), Vol. 1, p. 704.